phys. stat. sol. (b) **210**, 87 (1998)

Subject classification: 73.61.Ey; 63.20.Kr; S7.12

Mutual Hot-Phonon Effects in Coupled GaAs Quantum Wires

G. PAULAVIČIUS (a), R. MICKEVIČIUS (a), V. MITIN (a), V. KOCHELAP[1]) (a), M. A. STROSCIO (b), and G. J. IAFRATE (b)

(a) Wayne State University, Department of Electrical and Computer Engineering, Detroit, MI 48202, USA

(b) U.S. Army Research Office, P.O. Box 12211, Research Triangle Park, NC 27709, USA

(Received July 31, 1998)

Hot phonon effects on electron transport in coupled GaAs quantum wires embedded in AlAs have been investigated by a self-consistent Monte Carlo simulation. These results take into account optical phonon confinement within the GaAs region and localization at its boundaries which is caused by the presence of GaAs/AlAs heterointerfaces. Electrical confinement of electrons in several spatially separated quantum wire channels inside the GaAs region with common optical phonons (confined within the whole GaAs bar) is assumed. We have investigated numerically mutual interaction of electrons and phonons over a wide range of electric fields ($0 < E < 1000$ V/cm) and lattice temperatures ($30\,\mathrm{K} \leq T \leq 300\,\mathrm{K}$). We demonstrate that in a system of two quantum wires coupled through the common confined optical phonons, electron transport in one wire significantly affects electron transport in the second wire due to the presence of the strong mutual hot-phonon drag between these electron channels. This leads to a sufficient modification of the carrier velocity–field characteristics in the structures investigated.

1. Introduction

Nonequilibrium (hot) optical phonons [1 to 7] generated by hot-electron gases strongly affect electron transport phenomena in low-dimensional GaAs structures [1]. These effects become especially pronounced in GaAs/AlAs-heterostructure-based quantum wires (QWIs) due to considerable restrictions on the electron and phonon motion in this case. The confinement inside the GaAs region bounded by GaAs/AlAs heterointerfaces as well as the substantial difference in the optical phonon generation/decay times ($\approx$0.15 ps/(7 to 8) ps for GaAs) lead to a significant growth of the nonequilibrium optical phonon population. Moreover, the one-dimensional (1D) confinement of optical phonons in the GaAs QWIs results in a directed momentum [7, 8] that has a pronounced influence on 1D electron transport.

Hot phonon build-up in 1D systems is substantially stronger than in bulk materials and quantum wells for the same equivalent electron concentrations. The coupling with nonequilibrium optical phonons makes electron transport in QWIs strongly nonlinear.

It has been demonstrated [8] that in single QWIs hot-optical-phonon effects on electron transport are twofold. At room temperature hot optical phonons lead to a signifi-

[1]) Permanent address: Institute of Semiconductor Physics, National Academy of Sciences of Ukraine, Kiev 252650, Ukraine.

cant increase of electron drift velocity in the QWIs. This *hot-phonon drag effect* is due to the strongly asymmetric nonequilibrium phonon distribution in the structure at room temperature. Due to the forward-shifted (i.e., shifted against the electric field in the structure) electron distribution in momentum space, the nonequilibrium phonon population displays underpopulation at negative wave numbers and overpopulation (hot phonons) at positive wave numbers. As a result, phonon absorption for *forward* electron transitions (when negatively charged electron gains momentum against the electric field) is enhanced, whereas the absorption for *backward* transitions (when electron gains momentum in the electric field direction due to this scattering) is suppressed. Hence, the electron drift velocity and the low-field mobility *increase*. Hot-phonon drag is pronounced in QWIs; indeed, the electron mobility and drift velocity increase by more than 30% [8]. At temperatures around 30 K, when equilibrium phonon populations are negligible, diffusive heating of electrons by hot optical phonons dominates over hot-phonon drag and the electron drift velocity decreases.

Moreover, recent studies [9 to 11] of the dynamics of nonequilibrium electron–phonon systems in single quasi-one-dimensional quantum wires indicate that hot-phonon phenomena in such structures display some peculiarities not present in bulk semiconductors and quantum wells; as examples, nonequilibrium phonon build-up and the role of these phonons in electron relaxation depend strongly on the shape of the initial distribution of injected or photoexcited electrons [9 to 11].

Since the model for electron–phonon interactions in a single QWI is well established [8 to 13], the primary interest of our present study is the mutual interaction of similar QWI channels *coupled by a common optical phonon system*. We have developed and justified the model of such a structure based on the model of a single GaAs QWI. In the present paper these previous results are extended to the coupled wire structure through simulations of the interaction of electron and phonon systems as well as of *mutual hot-phonon drag effects* in the QWIs coupled by common optical phonons.

2. Model

We have investigated nonlinear electron transport and hot optical phonon system dynamics in coupled 150×250 Å^2 GaAs quantum wires formed by transverse electrical confinement in rectangular 450×250 Å^2 cross-section 1D GaAs bar embedded in AlAs. A schematic illustration of such a system is shown in Fig. 1.

The transverse confinement of longitudinal optical (LO) phonons inside the GaAs bar is assumed to obey the well-established dielectric continuum model [14, 15]. This bar may also serve as the electron confinement region as, e.g., in a single QWI. However, these carriers are additionally electrically separated into two smaller wire-like GaAs regions, electron channels Ch1 and Ch2 (as depicted in Fig. 1), by applying a negative potential to the gate G [16]. We assume that both of the QWI channels formed in this way have approximately *rectangular* cross-sections of 150×250 Å^2. This assumption does not hold in general for the "internal" (with respect to the GaAs region) boundaries of the QWI channels as indicated by the dashed lines in Fig. 1. However, our estimates using different electron wave functions, corresponding to more realistic shapes of the electrical electron confinement in the structure, show that the corrections are small. Indeed, the overlap of electron and phonon wave functions does not depend critically on the *exact* shape of electron wave functions. Therefore, for the

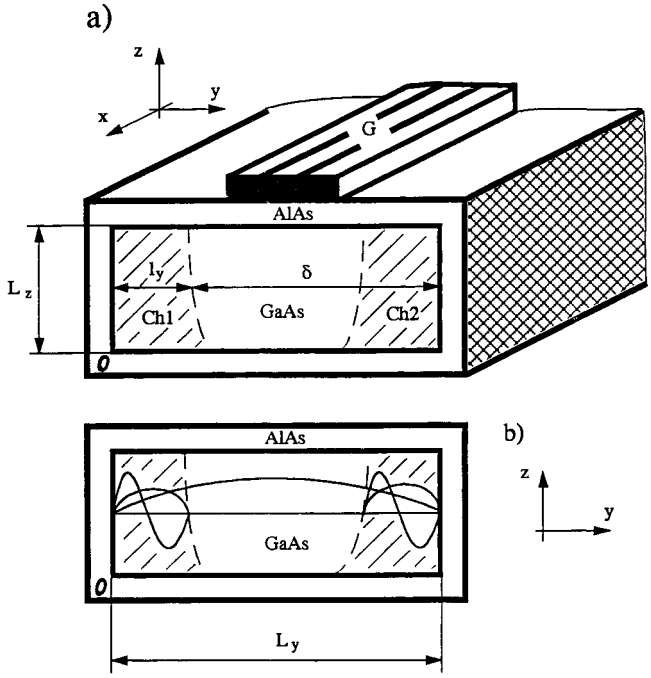

Fig. 1. a) Schematic illustration of a structure of two parallel QWI channels with common optical phonons. Dashed areas are cross-sections of 150×250 Å^2 1D electron channels (Ch1, Ch2). Electron confinement in these QWIs is achieved by the use of GaAs/AlAs heterointerfaces as well as by applying negative potential to the gate G. The phonons are confined within the 450×250 Å^2 rectangular cross-section GaAs bar. Coordinate system origin, point O, is located at the lower left-hand-side corner of the GaAs region; $l_y = 150$ Å and $L_y = 450$ Å are the electron and the optical phonon confinement lengths in y-direction, respectively, and δ stands for the distance between the phonon and electron confinement region edges; b) sinusoids in the structure cross-section represent the several lowest confined electron and optical phonon modes

sake of simplicity we present results obtained using QWI electron wave functions obtained for rectangular cross-section.

1D electron concentration is assumed to be uniform in the coupled QWIs and equal to 10^5 cm^{-1}; this linear density is appropriate for the case of nondegenerate electron gas in the range of longitudinal electric fields considered herein. We have used this electron concentration throughout all our simulations of this study except in the cases where another density is specified.

It is evident that for the structure shown in Fig. 1 the two parallel spatially separated 1D electron channels are *coupled* through *a common optical phonon system*. As shown in this figure, in y-direction the phonon confinement (450×250 Å^2 GaAs region) is different from electron confinement ($\approx 150 \times 250$ Å^2 channels (Ch1, Ch2)). Therefore, the optical phonon scattering rates in these 1D electron channels differ, in general, from those in the corresponding single QWIs [13]. This difference is caused by the electron and optical phonon wave function overlap integral in y-direction as discussed further in Appendix A. In the case when both the electron and optical phonon confinement lengths in the transverse directions (i.e., y and z) coincide, as in the case of a

single QWI, the overlap integral between electron and phonon wave functions, P_{rs}, is given by [13]

$$P_{rs} = \frac{1}{4\pi^2}\left[\frac{(-1)^{m+m'+r}-1}{m+m'+r} - \frac{(-1)^{m+m'-r}-1}{m+m'-r} - \frac{(-1)^{m-m'+r}-1}{m-m'+r} + \frac{(-1)^{m-m'-r}-1}{m-m'-r}\right] \times \left[\frac{(-1)^{n+n'+s}-1}{n+n'+s} - \frac{(-1)^{n+n'-s}-1}{n+n'-s} - \frac{(-1)^{n-n'+s}-1}{n-n'+s} + \frac{(-1)^{n-n'-s}-1}{n-n'-s}\right]. \quad (1)$$

Here m, n and m', n' stand for initial and final 1D electron state numbers, respectively, and r, s indicate optical phonon modes. In the case of different electron and phonon confinement in one transverse direction (e.g., in y-direction as in Fig. 1) the overlap integral becomes

$$P_{rs} = \frac{1}{4\pi^2}\left[\frac{\cos\left(\pi\left(m+m'+r\,\frac{l_y+\delta}{L_y}\right)\right) - \cos\left(r\pi\,\frac{\delta}{L_y}\right)}{m+m'+r\,\frac{l_y}{L_y}} - \frac{\cos\left(\pi\left(m+m'-r\,\frac{l_y+\delta}{L_y}\right)\right) - \cos\left(r\pi\,\frac{\delta}{L_y}\right)}{m+m'-r\,\frac{l_y}{L_y}} - \frac{\cos\left(\pi\left(m-m'+r\,\frac{l_y+\delta}{L_y}\right)\right) - \cos\left(r\pi\,\frac{\delta}{L_y}\right)}{m-m'+r\,\frac{l_y}{L_y}} + \frac{\cos\left(\pi\left(m-m'-r\,\frac{l_y+\delta}{L_y}\right)\right) - \cos\left(r\pi\,\frac{\delta}{L_y}\right)}{m-m'-r\,\frac{l_y}{L_y}}\right] \times \left[\frac{(-1)^{n+n'+s}-1}{n+n'+s} - \frac{(-1)^{n+n'-s}-1}{n+n'-s} - \frac{(-1)^{n-n'+s}-1}{n-n'+s} + \frac{(-1)^{n-n'-s}-1}{n-n'-s}\right]. \quad (2)$$

Appendix A presents an outline of the derivations of the results of Eqs. (1) and (2) as well as the corresponding transition probabilities.

As depicted in Fig. 1, the parameter δ in Eq. (2) denotes the distance between the boundaries of phonon and electron confinement regions (L_y and l_y, respectively). Let us notice that the above expression (2) is valid even if $l_y + \delta < L_y$, i.e., for the case when in y-direction the electron channel has an arbitrary position inside the phonon confinement region ($L_y \times L_z$ GaAs bar). In Eqs. (1) and (2) only LO phonon modes r and s which correspond to *non-zero denominators* are taken into account. Note that in Eq. (2) variables corresponding to the transverse directions with respect to the rectangular cross-section QWI axis are separated. In other words, the parameters in the first brackets, such as m, m', r represent electron and optical phonon confinement in y-direction and n, n', s in the second brackets correspond to the confinement in z-direction. It is easy to verify that Eq. (2) reduces to Eq. (1) in the case when the confinement length in y-direction is the same for both electrons and the phonons, i.e., $l_y = L_y$ and $\delta = 0$.

The contributions of different optical phonon modes are different in Eqs. (1) and (2). Indeed, unlike in single QWIs, in such complex structures the contribution of higher phonon modes to electron scattering may be greater than the contribution of the first confined mode. However, according to Eqs. (1) and (2) our results indicate that *the integral effect* of all these modes remains *almost the same* as can be seen in Fig. 2. In other words, the rate of electron scattering by LO optical phonons in the systems is not considerably different from that in single QWIs (see Fig. 2).

For the simulation of mutual hot-phonon effects in coupled QWIs we use an ensemble Monte Carlo method to solve coupled nonlinear kinetic equations for both electrons and phonons. In these simulations, we have modified electron–optical-phonon scattering rates in accordance with the results presented previously in this paper. As mentioned, the results presented were obtained using wave functions for rectangular cross-section QWIs. For the purpose of making semi-quantitative estimates of mutual hot-phonon effects, such an idealized model of common phonons is quite acceptable as demonstrated by our analysis.

Our model assumes an infinitely deep rectangular potential well for electrons at the 1D channel boundaries. Multi-subband parabolic electron energy band structure as well as electron intersubband and intrasubband scattering by optical and acoustic phonons are taken into account. LO phonons are treated as confined within the GaAs bar in accordance with the dielectric continuum model [14, 15] while acoustic phonons are assumed to be *bulk-like* [17]. The use of moderately thick QWIs in our simulation results in strongly diminished roles of acoustic-phonon scattering and electron intersubband transitions [9].

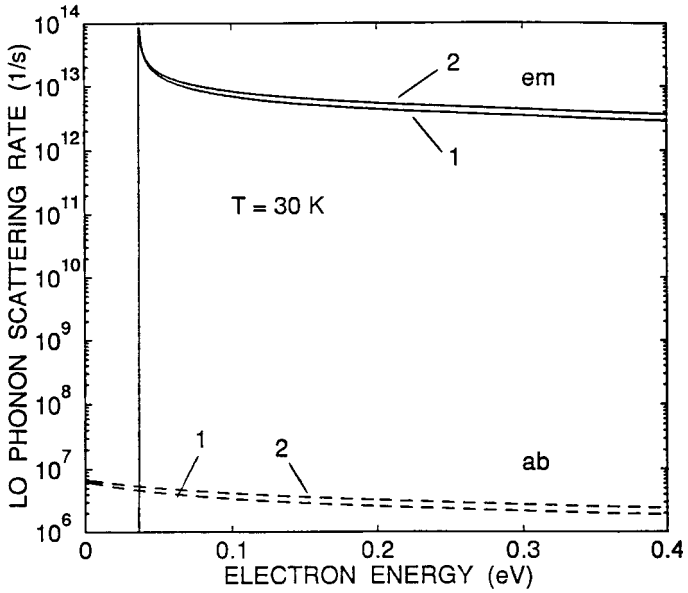

Fig. 2. Electron–optical-phonon scattering rate dependence on electron energy. Solid and dashed curves represent LO phonon emission and absorption, respectively. Curves 1 correspond to the case of a single QWI when the electron and phonon confinement lengths coincide in y-direction: $l_y = L_y = 150$ Å, $\delta = 0$. Curves 2 represent the case of coupled QWIs (Fig. 1) when $L_y = 150$ Å, $L_y = 450$ Å, and $\delta = 300$ Å

Due to their dominant coupling with electrons in medium to thick QWIs [18], only *nonequilibrium distributions* of confined longitudinal optical phonons are taken into account. The distributions of two branches of surface optical (SO) phonons, also known as interface phonons, are assumed to be in equilibrium. Hot LO phonons have been included using the procedure proposed in [5]. We have simulated two separate electron systems simultaneously keeping track of nonequilibrium phonon generation by both electron channels and updating the scattering rates accordingly [5, 7].

The nonequilibrium optical phonon thermalization (decay) time has been taken to be the same as in bulk GaAs, $\tau_d = 7$ ps, because the most complete existing model indicates that the decay time does not depend crucially on the dimensionality of the semiconductor structure [19]; this time constant is realistic for the conditions chosen. The inelasticity of acoustic-phonon scattering in QWIs [20] is also included in our model. We have considered relatively high temperatures (30 to 300 K); therefore, electron–electron intersubband scattering and electron scattering by regions of interface roughness have been neglected [21, 22].

All other model parameters have been chosen to be the same as for a single QWI [8, 12, 13, 18, 23].

3. Simulation Results

We have performed Monte Carlo simulations of electron transport in the coupled QWIs under nonequilibrium LO phonon conditions. In order to identify hot-phonon effects we have also calculated electron transport characteristics in the case of near-equilibrium phonons; the latter situation corresponds to low electron concentrations in the QWI channel.

Hot-phonon drag phenomena in a single QWI [8] clearly indicate that nonequilibrium optical phonons carry considerable directed momentum obtained from the heated electron system. This momentum can be transferred to another (coupled) carrier subsystem by means of common phonon re-absorption.

It must be noted that a similar Monte Carlo simulation of the mutual hot-phonon drag between parallel quantum wells (QWs) due to exchange of *acoustic phonons* has been reported recently [24]. That drag effect has been found to be rather small. In order to induce a current in a test QW, which is fifty times smaller than the driving current in parallel QWs, it was necessary to have more than ten *driving* QWs in parallel to one test QW. This is so because the acoustic phonons in such QW structures are bulk-like and their momentum is three-dimensional. Therefore, only the parallel component of the phonon momentum contributes to the drag effect. However, as has been shown in [25] and [26], in QWIs and QWs this parallel momentum component is negligible in comparison with the transverse component. Moreover, acoustic phonons can penetrate through the parallel electron channels faster than they can be absorbed by carriers. Nevertheless, the drag effect induced by nonequilibrium acoustic phonons is substantially stronger than the Coulomb drag [27]. In QWIs, the only free component of momentum for nonequilibrium *optical phonons* is the parallel one; hence, the total phonon momentum contributes to the drag effect. As a result, the drag effects should be much better pronounced relative to those in QWs and bulk materials.

We have simulated *the mutual hot-phonon drag effect* in two parallel *coupled* QWIs. Electron concentrations in both channels have been taken to be equal; more specifi-

cally, $n_1 = n_2 = 10^5\ \mathrm{cm}^{-1}$. The electric field is applied only to the *driving* QWI. Figs. 3a and b depict electron velocities in *driving* and *drag* channels versus electric field in the driving QWI at $T = 30$ K and 300 K, respectively. To compare the results obtained we plot two additional curves on each graph. Those solid curves, 1 and 2, correspond to v–E characteristics of a single QWI (having identical geometry and parameters as the coupled electron channels) without and with hot phonons, respectively. Note that in Figs. 3a and b the relative position of these two curves changes: curve 2 (hot phonons

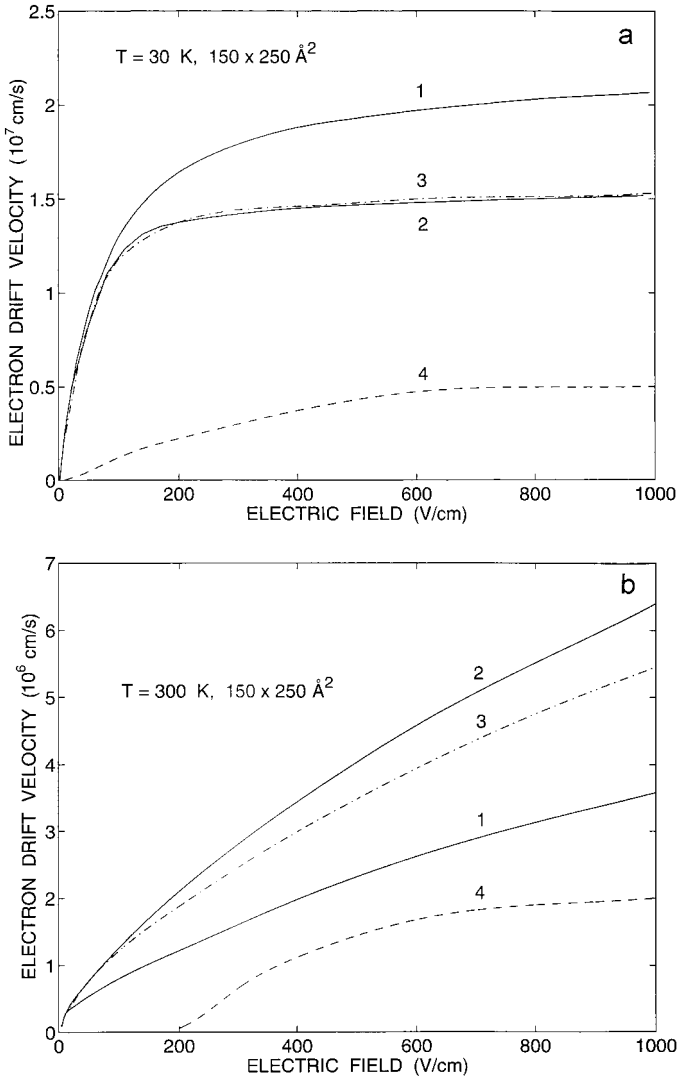

Fig. 3. Electron drift velocity in two coupled QWIs versus electric field in the driving channel: a) $T = 30$ K, b) $T = 300$ K. Single QWI: curves 1 represent the drift velocity without hot phonons, curve 2 with hot phonons taken into account. Coupled QWIs: curves 3 represent electron drift velocity in the channel with the electric field (drive velocity), curves 4 represent the drift velocity in the channel without electric field (drag velocity)

taken into account), being below curve 1 (hot phonons neglected) for 30 K, shifts above it for 300 K. Those trends are in accordance with the fact that nonequilibrium optical phonons have a different influence on electron mobility at low and high lattice temperatures [8].

From Fig. 3 it is clear that the electron drift velocity in the drag QWI, where the drag determines the carrier velocity (dashed curves 4), reaches almost 30% of the drive velocity (dash-dotted curves 3); i.e., the mutual hot-phonon drag effect is strongly pronounced in the structure. The existence of the drag channel does not affect the drive velocity at $T = 30$ K, whereas it affects this velocity at $T = 300$ K; this is evident comparing curves 3 and 2 in Figs. 3a and b. Physically, these trends occur because the hot-phonon occupation number is much larger (less spread and higher peaked) at $T = 30$ K and, therefore, it is affected less by hot-phonon re-absorption in the drag channel; the drive velocity (curve 3) is almost the same as electron drift velocity in an identical single QWI (curve 2 in Fig. 3a). At $T = 300$ K the presence of the drag channel leads to considerable modification of the nonequilibrium optical phonon distribution in the structure and causes a decrease in the drive velocity with respect to the electron drift velocity in a single QWI; this is illustrated by curves 3 and 2 in Fig. 3b.

The system of two QWIs coupled by common phonons and biased by *opposite* electric fields is interesting physically and exhibits unique velocity–field characteristics. If the doping level in such QWIs is *sufficiently different*, e.g., $n_1 \gg n_2$, optical phonons accumulated by electrons in the first electron channel prevail in determining the properties of the system. The contribution of the second QWI to hot-phonon build-up is negligible. In other words, in the common nonequilibrium optical phonon distribution there is a pronounced domination of the phonons with wave vectors oriented oppositely to the electric field direction of the QWI with the higher doping level. The situation can be interpreted as if the slightly doped electron channel is placed into the strong "external" phonon flux directed against this QWI's "internal" electric field. On the other hand, electrons in the first higher doped QWI channel practically do not experience the presence of the other channel due to insufficient phonon accumulation as well as re-absorption by electrons in the latter lower doped electron channel. From this consideration it follows that the v–E characteristic of such a coupled QWI system is substantially asymmetric.

Figs. 4a and b show the electron drift velocity dependencies on the magnitude of the electric field in the two channels (curves 1 and 2) for 30 and 300 K, recpectively; here we have plotted the absolute values of the drift velocities versus electric field magnitude in the corresponding electron channel keeping in mind that the actual fields and the carrier velocities are *opposite* in the two QWIs. The electron concentration in the first channel was chosen as $n_1 = 10^5\ \mathrm{cm}^{-1}$. This value is much higher than that in the second channel: $n_2 < 10^4\ \mathrm{cm}^{-1}$. The electron drift velocity in the higher doped first channel (dashed curves 1) is obviously the same as that in a single QWI [8]. As discussed, the second channel does not affect hot-phonon build-up and electron transport in the first channel. The drift velocity in the second channel (curves 2, Fig. 4) is considerably lower because electrons in the second channel move "against" the flow of the hot phonons generated by electrons in the first channel. Moreover, due to the fact that the nonequilibrium phonon population generated by electrons in the first channel grows linearly with increasing electric field [8], so does their influence on electron transport in the second channel. As result, the electron drift velocity in channel 2 almost

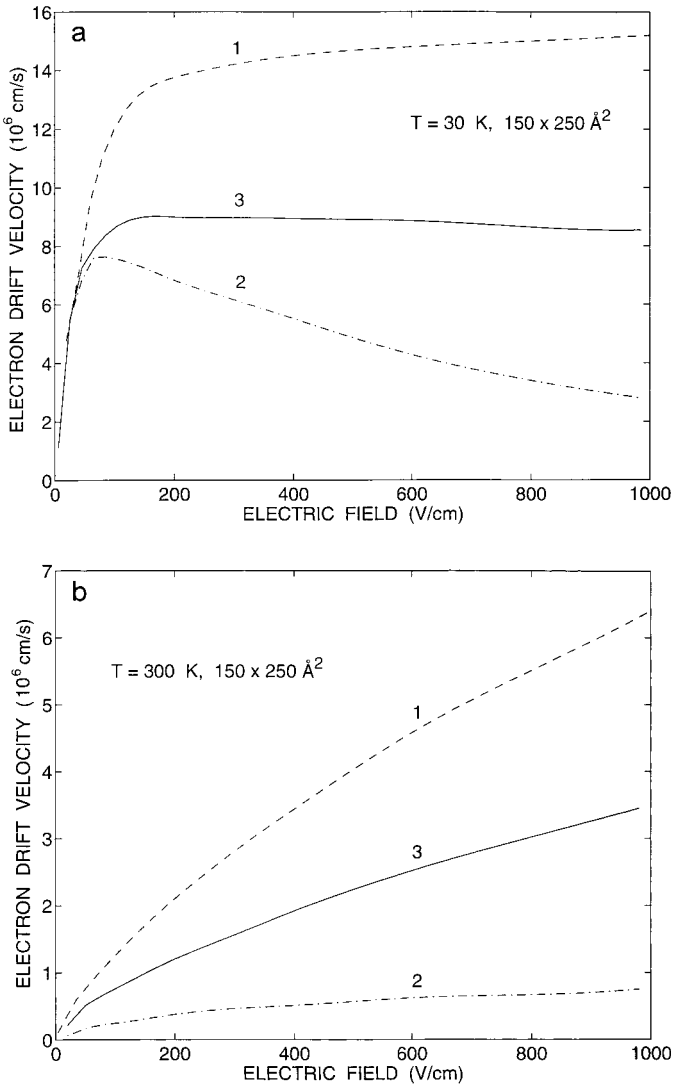

Fig. 4. Electron velocity–field characteristics in parallel QWIs coupled through the common optical phonon system: a) $T = 30$ K, b) $T = 300$ K. Electric fields and electron drift velocities in channels 1 and 2 have opposite directions. Curves 1 and 2 represent the drift velocities in channels 1 and 2, respectively, when electron concentration in channel 1 is much greater than that in channel 2, $n_1 = 10^5$ cm$^{-1} \gg n_2 < 10^4$ cm^{-1}. Curve 3 represents electron drift velocity in either channel, when $n_1 = n_2 = 10^5$ cm^{-1}

saturates at $T = 300$ K (Fig. 4b) and it even decreases at $T = 30$ K as the electric field increases (Fig. 4a).

Fig. 4 also reveals similar v–E dependences for two *identical* coupled QWIs biased by opposite electric fields. In this case, electron concentrations in both electron channels are *the same*, i.e., $n_1 = n_2 = 10^5$ cm^{-1}. The drift velocities (curves 3 in Figs. 4a and b)

are also of the same magnitude but of opposite directions. At a temperature of 30 K, Fig. 4a, there is a slightly pronounced negative differential mobility on curve 3.

As is seen from Fig. 4, the electron drift velocity in the symmetrical coupled electron channel system (curves 3) is lower than that in the corresponding higher doped QWI of the asymmetric structure (curves 1); this result holds for both temperatures. Such a difference is caused by the carrier coupling with the oppositely directed "foreign" phonon flux accumulated by the other QWI. At the same time this velocity is larger than that in the channel with a lower level of doping of the asymmetric QWI structure. This occurs as a result of the symmetry of the structure which ensures the phonons in neither channel dominate in the common optical phonon distribution in this case.

In concluding, we would like to pay attention to one interesting nonlinear transport phenomenon which could be caused by the phonon drag effect. The strongly asymmetric shape of velocity–field characteristics in two differently doped coupled QWIs with *opposite* electric fields suggests the possibility of *bistable electron transport* in this system when the electron concentrations are equal in both electron channels. Qualitatively such a possibility can be explained as follows. Any fluctuation of phonon population in the system leads to a change in the drift velocity in both channels. For definiteness let us assume that electrons in the first channel have a positive drift velocity and the carriers in the second channel have a negative velocity. Let us consider a common hot optical phonon fluctuation characterized by a decrease of phonons with positive wave numbers. As a result, the electron drift velocity in the second channel will increase (they are moving "against" the momentum of such phonons). Consequently, the phonon population with negative wave numbers, which is generated predominantly by electrons in the second QWI, will increase and will cause a decrease of the electron drift velocity in the first channel. This decrease in electron drift velocity in the first channel will lead to a further decrease in the phonon population with positive wave numbers, etc. If the mutual influence of electron transport in each channel is sufficiently strong, this process will lead to the situation indicated by curves 1 and 2 in Fig. 4, where the first channel does not contribute to the phonon generation and, therefore, does not affect electron transport in the second electron channel. The strength of the mutual influence of two identical coupled electron channels is determined by the dependence of the nonequilibrium phonon population on the electron drift velocity (at fixed electric field).

However, the accurate investigation of this phenomenon would require more detailed quantum-mechanical approach adequate for the description of time evolution of electron–phonon system. We stress that in the present paper we consider the QWI structure under steady state; our electrons interact with already established stationary confined optical phonon distribution. The analysis of the transient stage (processes of propagation of the emitted phonons in the transverse directions before the standing waves are established) is out of scope of our paper. Note that for the transient stage it is natural to expect that if electron channels are separated by a distance l, mutual drag effects are scaled by a factor $\exp(-l/L_{\mathrm{ph}})$, where $L_{\mathrm{ph}} = |\mathrm{d}w/\mathrm{d}k|\,\tau_{\mathrm{ph}}$ is the distance an optical phonon propagates before decaying into acoustic phonons. However, at steady state the phonon propagation time does not play a significant role and the spatial dependence comes from the form-factor represented by the overlap integral of electron and phonon wave functions.

It should be pointed out that the mentioned hot-phonon drag effect in the coupled QWI system can find its application in a variety of novel nanoscale devices [28].

4. Summary

By employing the ensemble Monte Carlo technique we have investigated electron transport in coupled quantum wires under nonequilibrium optical phonon conditions.

Our treatment of coupled-wire channels is not aimed at an accurate quantitative description; rather, it provides semi-quantitative estimates for the phenomena being studied. A simplification has been made when considering electron transport in the QWI structures investigated; specifically, it has been assumed that the two QWIs have *common* LO phonons. As discussed, such a situation can be realized in QWIs with combined lattice and electrical confinement of electrons. Obviously, the phonons in such structures are different from those in single QWIs bounded by heterointerfaces. However, for the purpose of making estimates this idealized model is appropriate, since, as demonstrated, the total electron scattering rates are not affected crucially by phonon confinement in one or two directions.

In QWIs coupled through a common phonon system, electron transport in one QWI significantly affects electron transport in the second QWI. If only one QWI is biased by an electric field, it serves as a driving channel for another unbiased QWI (drag channel). The effect of induced velocity in an unbiased QWI results from the mutual hot-phonon drag effect and is pronounced in QWIs. The electron drift velocity in the drag channel reaches more than 30% of the magnitude of the driving velocity. If electron concentrations are significantly different in the two channels, the velocity–field characteristics become strongly asymmetric. The asymmetric velocity–field characteristic implies the possibility of a bistable transport regime.

Appendix A

Nonequilibrium optical phonons in coupled quantum wire systems

Let us consider in more detail electron–optical-phonon scattering rates when there is confinement of both these quasiparticles in one direction, e.g., y, is different as indicated in Fig. 1. Here we follow the approach used in [13] and [15].

Assume that electron motion is allowed only in x-direction (longitudinal in respect to QWI axis) and is strictly quantized in both transverse y and z-directions. The same situation is valid for confined LO phonons as well. However, in the y-direction the former quasiparticles are confined electrically in the conducting channels (Ch1, Ch2) while the phonons are confined in the whole GaAs region (see Fig. 1). Let us denote the characteristic size of electron confinement by l_y and that of phonons L_y ($l_y < L_y$). For simplicity, we assume that the cross-sections of the quasiparticle confinements have *rectangular shapes.*

The electron wave function for the case of infinite well potentials at the QWI conducting channel boundaries of the structure considered has the following well-known form:

$$|k_x, m, n\rangle = \frac{1}{\sqrt{L_y}} \exp(ik_x x) \sqrt{\frac{2}{l_y}} \sin\left(\frac{m\pi y}{l_y}\right) \sqrt{\frac{2}{L_z}} \sin\left(\frac{n\pi z}{L_z}\right), \tag{A1}$$

for Ch1 (i.e., for $0 \le y \le l_y$ and $0 \le z \le L_z$) in Fig. 1. Here $m = 1, 2, \ldots$ and $n = 1, 2, \ldots$ denote the electron energetic subband numbers and k_x is the x-component of electron

wave vector corresponding to the direction of the free motion. Note that $|k_x, m, n\rangle = 0$ when $y > l_y$ or $y < 0$. The similar expression can be written for the confined optical phonon modes in the structure according to the dielectric continuum model [14],

$$|q_x, r, s\rangle = \frac{1}{\sqrt{L_x}} \exp(iq_x x) \sqrt{\frac{2}{L_y}} \sin\left(\frac{r\pi y}{L_y}\right) \sqrt{\frac{2}{L_z}} \sin\left(\frac{s\pi z}{L_z}\right). \tag{A2}$$

Here $0 \le y \le L_y$ and $0 \le z \le L_z$ as illustrated in Fig. 1.

Assuming that the Fermi Golden rule provides an accurate evaluation of the electron transition probabilities in momentum space, let us calculate 1D electron scattering rates due to interaction with confined LO optical phonons. The transition probability of an electron being scattered from an initial state $|k_x, m, n\rangle$ to a final state $|k'_x, m', n'\rangle$ in this case can be written down as follows:

$$\lambda^{e/a}(k_x, m, n; k'_x, m', n') = \frac{2\pi}{\hbar} |M^{e/a}|^2 \delta[\varepsilon(k'_x, m', n') - \varepsilon(k_x, m, n) \pm \hbar\omega_{LO}]. \tag{A3}$$

The superscripts "e" and "a" and the plus and minus signs indicate optical phonon emission and absorption, respectively; the δ-function in the expression stands for energy conservation in the process under consideration; ε and $\hbar\omega_{LO}$ are electron and LO phonon energies, respectively.

The matrix element for the electron–optical-phonon interaction, $M^{e/a}$, has the following form:

$$M^{e/a} = \left\langle k'_x, m', n'; N + \frac{1}{2} \pm \frac{1}{2} |H^{1D}| k_x, m, n; N + \frac{1}{2} \mp \frac{1}{2} \right\rangle, \tag{A4}$$

where H^{1D} is the Fröhlich Hamiltonian [13] of the 1D confined longitudinal optical phonons.

The total electron scattering rate from the state $|k_x, m, n\rangle$ to elsewhere can be obtained by summing Eq. (A3) over all possible final electron states,

$$\begin{aligned} \Lambda^{e/a}(k_x, m, n) &= \sum_{k'_x, m', n'} \lambda^{e/a}(k_x, m, n; k'_x, m', n') \\ &= \sum_{m', n'} \frac{e^2}{8\pi^2\varepsilon_0} \int dq_x \omega_{LO}(N + 1/2 \pm 1/2) \\ &\quad \times I_{LO}(q_x, l_y, L_z) \delta[\varepsilon(k'_x, m', n') - \varepsilon(k_x, m, n) \pm \hbar\omega_{LO}] \delta_{k'_x, k_x \pm q_x}, \end{aligned} \tag{A5}$$

where I_{LO} is the electron–optical-phonon coupling factor and m', n' denote the final electron subband numbers. In this expression q_x stands for the emitted/absorbed optical phonon wave vector x-component; e and ε_0 represent the electron charge and the vacuum dielectric permittivity, respectively.

The coupling factor I_{LO} can be expressed as

$$I_{LO}(q_x, l_y, L_z) = \left(\frac{1}{\varkappa_\infty} - \frac{1}{\varkappa_0}\right) \frac{2\pi^2}{l_y L_z} \sum_{r=1,2,3,\ldots} \sum_{s=1,2,3,\ldots} \left[\frac{4P_{rs}}{\sqrt{q_x^2 + \left(\frac{r\pi}{l_y}\right)^2 + \left(\frac{s\pi}{L_z}\right)^2}}\right]^2. \tag{A6}$$

Here $\varkappa_0$ and $\varkappa_\infty$ are low and high frequency GaAs permittivities, respectively, and P_{rs} stands for the overlap integral between the electron and LO phonon wave functions. In the case, when these functions are as those in Eqs. (A1) and (A2), P_{rs} takes the form of Eq. (2).

References

[1] M. Lax and W. Cai, Internat. Mod. J. Phys. B **6**, 171 (1992).
[2] P. Kocevar, J. Phys. C **5**, 3349 (1972).
[3] P. Kocevar, Physica **134B**, 155 (1985).
[4] P. Lugli, C. Jacoboni, L. Reggiani, and P. Kocevar, Appl. Phys. Lett. **50**, 1251 (1987).
[5] R. Mickevičius and A. Reklaitis, Solid State Commun. **64**, 1305 (1987).
[6] L. Hlou, J. C. Vaissiere, J. P. Nougier, L. Varani, P. Houlet, L. Reggiani, M. Fadel, and P. Kocevar, in: Proc. 3rd Internat. Workshop Comp. Electron, Ed. S. M. Goodnick, Oregon State University, Portland, OR, 1994 (p. 49).
[7] V. V. Mitin, G. Paulavičius, and N. A. Bannov, Nonlinear Electron–Optical Phonon Coupled Transport in Double-Barrier GaAs/AlAs Quantum Well, accepted for publication in Superlattices and Microstructures.
[8] R. Mickevičius, V. Mitin, G. Paulavičius, V. Kochelap, M. A. Stroscio, and G. J. Iafrate, Hot-Phonon Effects on Electron Transport in Quantum Wires, accepted for publication in J. Appl. Phys.
[9] R. Gaška, R. Mickevičius, V. Mitin, M. A. Stroscio, G. J. Iafrate, and H. L. Grubin, J. Appl. Phys. **76**, 1 (1994).
[10] R. Mickevičius, R. Gaška, V. Mitin, M. A. Stroscio, and G. J. Iafrate, Semicond. Sci. Technol. **9**, 889 (1994).
[11] L. Rota, F. Rossi, P. Lugli, and E. Molinari, Semicond. Sci. Technol. **9**, 871 (1994).
[12] D. Jovanovic, J. P. Leburton, and K. Ismail, Semicond. Sci. Technol. **9**, 882 (1994).
[13] K. W. Kim, M. A. Stroscio, A. Bhatt, R. Mickevičius, and V. V. Mitin, J. Appl. Phys. **70**, 319 (1991).
[14] N. Mori and T. Ando, Phys. Rev. B **40**, 6175 (1989).
[15] M. Stroscio, Phys. Rev. B **40**, 6240 (1989).
[16] C. Weisbuch and B. Vinter, Quantum Semiconductor Structures. Fundamentals and Applications, Academic Press, Boston 1991.
[17] F. T. Vasko, Soviet Phys. – Solid State **30**, 1207 (1989).
[18] R. Mickevičius, V. V. Mitin, K. W. Kim, M. A. Stroscio, and G. J. Iafrate, J. Phys.: Condensed Mater **4**, 4959 (1992).
[19] G. Mahler, A. M. Kriman, and D. K. Ferry, unpublished.
[20] R. Mickevičius, V. V. Mitin, U. K. Harithsa, D. Jovanovic, and J. P. Leburton, J. Appl. Phys. **75**, 973 (1994).
[21] J. P. G. Taylor, K. J. Hugill, D. D. Vvedensky, and A. MacKinnon, Phys. Rev. Lett. **67**, 2359 (1991).
[22] J. A. Nixon and J. H. Davies, Phys. Rev. B **41**, 7929 (1990).
[23] R. Mickevičius and V. V. Mitin, Phys. Rev. B **48**, 17194 (1993).
[24] M. Mosko, J.-L. Pelouard, and F. Pardo, Semicond. Sci. Technol. **9**, 806 (1994).
[25] V. V. Mitin, G. Paulavičius, and N. A. Bannov, J. Appl. Phys. **79**, 8955 (1996).
[26] R. Mickevičius, V. V. Mitin, V. Kochelap, M. A. Stroscio, and G. J. Iafrate, J. Appl. Phys. **77**, 5095 (1995).
[27] T. J. Gramila, J. P. Eisenstein, A. H. MacDonald, L. N. Pfeiffer, and K. L. West, Phys. Rev. Lett. **66**, 1216 (1991).
[28] V. Mitin, V. Kochelap, R. Mickevičius, M. Dutta, and M. A. Stroscio, patent pending.